Editors' Suggestion

Dissipative Kerr soliton self-balancing from Kerr-induced synchronization

Pradyoth Shandilya [1], Kartik Srinivasan [2,3], Curtis Menyuk [1], and Grégory Moille [2,3,*]
[1] *University of Maryland, Baltimore County, Baltimore, Maryland 21250, USA*
[2] *Microsystems and Nanotechnology Division, National Institute of Standards and Technology, Gaithersburg, Maryland 20899, USA*
[3] *Joint Quantum Institute, NIST/University of Maryland, College Park, Maryland 20742, USA*

(Received 11 May 2026; accepted 15 September 2026; published 13 October 2026)

Integrated frequency-comb sources are a key enabling technology for frequency-metrology applications. Their on-chip integration promises to bring metrology capacity outside of the laboratory, particularly since they can operate at low continuous-wave pump laser power in the dissipative Kerr soliton (DKS) regime. Yet such a small footprint and low power come at a cost: higher noise and overall lower comb power. In particular, this translates to highly challenging detection and locking of the carrier-envelope offset, which is necessary for complete stabilization of the comb. Recently, Kerr-induced synchronization (KIS) of a DKS to a reference laser was demonstrated as a tool for passive all-optical stabilization of DKS microcombs, with fundamental modification to the DKS and microcomb properties. Here, we demonstrate that the combination of additional power from the reference laser (now part of the DKS) and the KIS phase locking that pins the repetition rate together fundamentally alters the DKS, forcing an energy redistribution to maintain its center of mass. We demonstrate this self-balancing effect theoretically, which in a pure quadratic dispersion resonator leads to reference-dependent recoil. With higher-order dispersion through which the DKS generates phase-matched dispersive waves (DWs), we show that self-balancing results in the enhancement of the high-frequency DW power, offering an all-optical pathway for efficient carrier-envelope-offset detection in octave-spanning microcombs.

DOI: 10.1103/921d-nf7h

I. INTRODUCTION

Optical frequency combs based on dissipative Kerr solitons (DKSs) in microresonators have emerged as low-power [1], mass-scale fabrication-compatible [2,3], and versatile coherent light sources for metrology [4,5], communications [6], spectroscopy [7], distance ranging [8], and other applications. However, like table-top counterparts, these microcombs require complete stabilization for metrological applications, typically involving detection and locking of their carrier-envelope-offset (CEO) frequency. Yet their low pump power and small footprint directly translate into low power per comb tooth and larger thermo-optic noise [9], leading to a poor signal-to-noise ratio [10] in nonlinear $f-2f$ interferometry for CEO detection [11]. Overcoming this limitation is essential for advancing field-deployable microcomb systems that combine broad spectral coverage with high coherence. A promising pathway towards such control is Kerr-induced synchronization (KIS) [12], in which a second laser injected into the same microresonator housing the DKS phase synchronizes the soliton [13], enabling passive stabilization and capture of a comb tooth. Thus, KIS provides a mechanism for passive two-point external control of the DKS microcomb to achieve ultralow-noise operation [14]. This ultralow-noise performance results from a fundamental modification of the DKS dynamics under KIS, breaking its symmetry to bypass intracavity noise and alter tooth-to-tooth noise propagation [15].

Previous investigations of KIS primarily focused on how the injection of a reference laser modifies the DKS repetition rate [12,16,17] and the resulting improvements in noise performance and passive stabilization [14,15]. What has remained largely unexplored, however, is how the injection of the reference laser fundamentally alters the energy dynamics of the DKS itself, specifically how the intracavity energy distribution and spectral symmetry of the soliton respond to the asymmetric power injection. Furthermore, prior theoretical treatments were largely confined to the case of pure quadratic dispersion [17,18], leaving the question of how higher-order dispersion terms which govern the formation of dispersive waves (DWs) and strongly modify spectral energy dynamics interact with KIS-induced energy redistribution as an open and important problem. In this work, we demonstrate that, by constraining the soliton's group velocity through the fixed frequency difference between the two optical pumps, KIS introduces a new degree of freedom in controlling the intracavity energy flow and spectral symmetry of the soliton state. We reveal that under KIS, the DKS undergoes a self-balancing process that restores its spectral center of mass (SCM) to the mode pumped by the main pump, compensating for the asymmetric energy injected by the reference pump on one side of the spectrum. Through a perturbative analysis of the multipump Lugiato-Lefever equation (MLLE) [16], supported by numerical simulations, we show that the soliton experiences a compensating spectral recoil directed opposite to the reference frequency [Figs. 1(a)–1(c)], effectively redistributing energy within the comb to maintain its spectral equilibrium. Importantly, this mechanism, which we term soliton self-balancing, has no

*Contact author: gmoille@umd.edu

 ©2026 American Physical Society

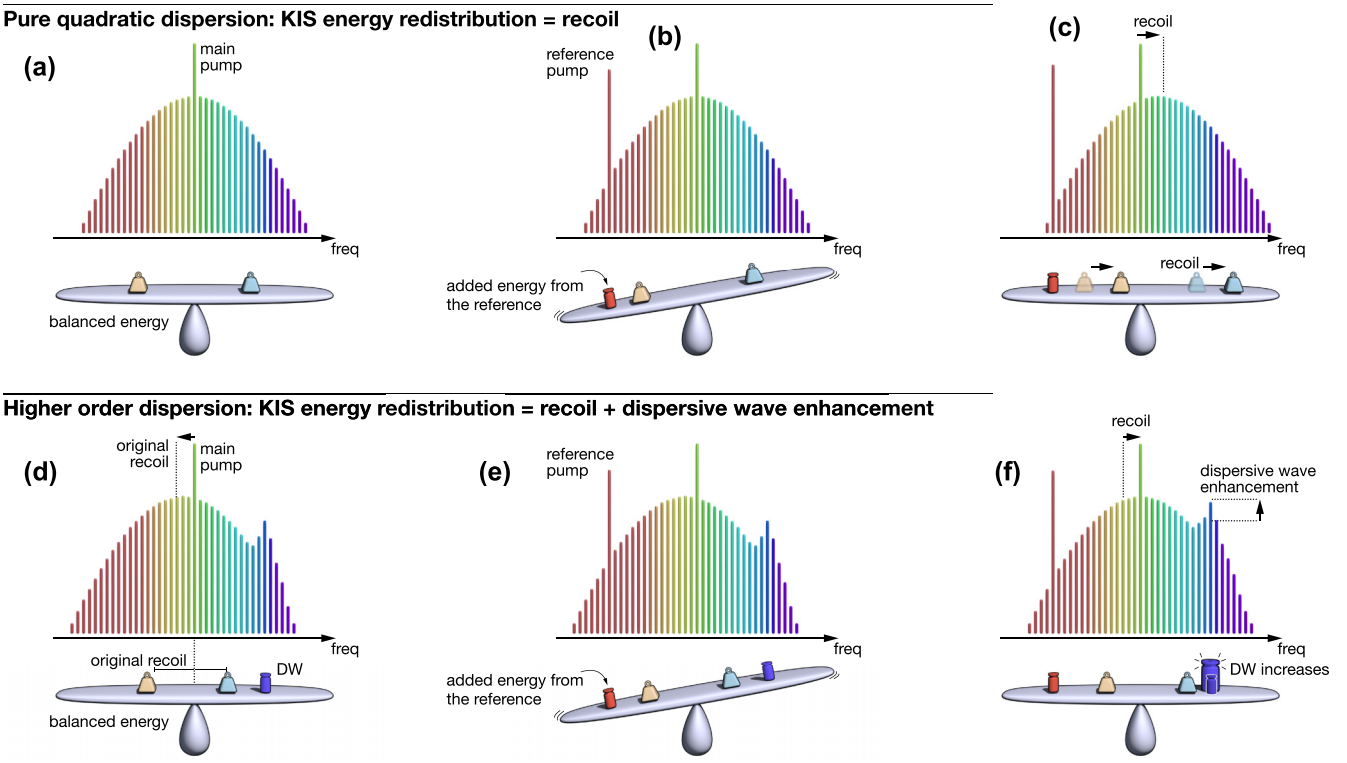


FIG. 1. Soliton self-balancing mechanism through spectral energy redistribution under Kerr-induced synchronization. (a)–(c) Pure quadratic dispersion case. (a) The DKS frequency comb centers on the main pump. The equivalent lever diagram represents conservation of the center of mass, which in the single-pump case corresponds to equal weight at equal distance from the center (i.e., the main pump). (b) In the KIS regime, however, the reference pump becomes part of the DKS and adds asymmetric energy, creating a nonphysical imbalance. (c) Because the repetition rate is pinned by the main and reference pumps, the DKS cannot compensate for the energy imbalance through temporal drift. The sole degree of freedom available to the DKS is to shift its center of mass, resulting in recoil. (d)–(f) Higher-order dispersion case. (d) If the resonator exhibits at least a tertiary dispersion term, the DKS becomes phase matched to at least one azimuthal mode of the cavity, leading to dispersive wave emission and creating a natural imbalance and hence an intrinsic recoil for center-of-mass conservation. (e) Similarly, in the KIS regime the reference pump adds an energy imbalance. (f) The DKS now possesses another degree of freedom to compensate for the reference energy. While it still compensates via recoil, it also increases its dispersive wave emission, enhancing the dispersive wave mode away from the reference mode. DW: dispersive wave.

analog in conventional single-pumped systems. Systems undergoing recoil from either higher-order dispersion [19,20] or Raman scattering [21–23] exhibit both spectral and temporal recoil because one follows from the other and, with appropriate engineering, they can cancel one another [23,24]. In contrast, our KIS system decouples these effects. The spectral recoil results from spectral reequilibration, whereas optical trapping of the DKS fixes the repetition rate. Moving beyond the case of pure quadratic dispersion, we further show that in systems with higher-order dispersion, self-balancing can transfer significant energy into a DW on the opposite side of the spectrum from the reference pump, resulting in a power enhancement of high-frequency DWs [Figs. 1(d)–1(f)]. The concept of soliton self-balancing intuitively extends the understanding of how KIS results in a redistribution of DKS spectral energy in systems with any order of dispersion. By linking KIS, spectral recoil, and DW dynamics, our findings reveal an energy reorganization behavior that can potentially be harnessed for engineered spectral control in chip-scale platforms.

II. SELF-BALANCING IN PURELY QUADRATIC DISPERSION RESONATORS

In the simplest system where the resonator exhibits only quadratic dispersion, the DKS follows a hyperbolic-secant-squared-like envelope that is perfectly symmetric about the main pump, without recoil. Consequently, the output state produces a frequency comb with repetition rate ν_{rep}^{0} that is exactly symmetric about the primary pump. Equivalently, its spectral center of mass coincides with the pumped mode [Fig. 1(a)]. KIS of the DKS from a second injected laser on either side of the main pump causes the in-phase component of the intracavity reference field to merge with the DKS. Hence, it leads to a displacement of the SCM towards the reference laser azimuthal mode [Fig. 1(b)]. However, due to the optical trapping of the DKS inside the potential created by the modulation between the main and reference pumps, its group and phase velocities are now entirely pinned by these two laser frequencies such that $\nu_{\mathrm{rep}}^{\mathrm{KIS}} = (\nu_{\mathrm{pmp}} - \nu_{\mathrm{ref}})/M$, where $\nu_{\mathrm{rep}}^{\mathrm{KIS}}$ is the disciplined soliton repetition rate, ν_{pmp} and

ν_{ref} are the main and reference pump frequencies, and M is the number of modes separating the two pumps. When at the center of the KIS window, namely, $\nu_{\mathrm{ref}} = \nu_{\mathrm{pmp}} + M\nu_{\mathrm{rep}}^{0}$, where the reference pump frequency exactly matches the frequency of one of the comb lines before KIS, there is no change in the repetition rate before and after KIS ($\nu_{\mathrm{rep}}^{0} = \nu_{\mathrm{rep}}^{\mathrm{KIS}}$), even though more power has been injected into the microresonator asymmetrically with respect to the main pump frequency. We therefore define the self-balancing effect as the redistribution of intracavity spectral energy that restores the spectral center of mass, consistent with the conservation of the DKS momentum [16,17], after asymmetric energy injection by the reference pump under the fixed group velocity and repetition rate imposed by KIS. With only quadratic dispersion available, the sole route to restore the spectral center of mass is a compensating spectral recoil away from the reference pump frequency [Fig. 1(c)]. Moving next to the case when higher-order dispersion is present, the possibility of phase matching between the cavity resonances and the soliton exists, leading to the creation of DW(s) [25–30], which will cause both a spectral and a temporal recoil [20,31] in the single-pump case [Fig. 1(d)]. Therefore, the addition of the reference pump leads to the same energy imbalance as in the pure quadratic dispersion case [Fig. 1(e)], introducing yet another degree of freedom to enable self-balancing. The dispersive radiation from the soliton can increase, leading to an enhancement of the DW opposite to the reference in the optical spectrum [Fig. 1(f)]. We study the latter case in the next section; in this section, we begin our study of soliton self-balancing in the simplest possible system to gain physical insight: a microresonator exhibiting purely quadratic dispersion.

The impact of the reference pump on the DKS spectral energy distribution can be analyzed using standard soliton perturbation theory [32–34], which has been successfully used to study soliton dynamics in microresonators [35,36]. The soliton dynamics in microresonators pumped by two lasers is described using the loss-normalized MLLE [15,16]:

$$\frac{\partial a}{\partial t} = -(1 + i\alpha_{\mathrm{pmp}})a + i\sum_{\mu} D_{\mathrm{int}}(\mu)A(\mu)e^{i\mu\theta} + i|a|^2 a + F_{\mathrm{pmp}} + F_{\mathrm{ref}}e^{i(\alpha_{\mathrm{ref}} - \alpha_{\mathrm{pmp}} + D_{\mathrm{int}}(\mu_{\mathrm{ref}}))t + i\mu_{\mathrm{ref}}\theta}, \quad (1)$$

where a is the intracavity field amplitude, A is its Fourier transform, t is time, θ is the azimuthal coordinate, α_{pmp} (α_{ref}) is the detuning of the primary (reference) pump with corresponding amplitude F_{pmp} (F_{ref}), D_{int} is the integrated dispersion as a function of the relative mode number μ, and μ_s is the relative mode number of the reference pump. If we consider only up to second-order dispersion, Eq. (1) reduces to

$$\frac{\partial a}{\partial t} = -(1 + i\alpha_{\mathrm{pmp}})a + iD_2\frac{\partial^2 a}{\partial\theta^2} + i|a|^2 a + F_{\mathrm{pmp}} + F_{\mathrm{ref}}e^{i[\alpha_{\mathrm{ref}} - \alpha_{\mathrm{pmp}} + D_{\mathrm{int}}(\mu_{\mathrm{ref}})]t + i\mu_{\mathrm{ref}}\theta}, \quad (2)$$

where D_2 is the second-order dispersion coefficient. Normalizing Eq. (2) with respect to the detuning following [35], with further details described in the Supplemental Material [37] (which also includes Ref. [38]), we obtain

$$\frac{\partial\psi}{\partial t} = -\left(\delta + \frac{i}{2}\right)\psi + \frac{i}{2}\frac{\partial^2\psi}{\partial x^2} + i|\psi|^2\psi - \frac{i}{2}h_{\mathrm{pmp}} - \frac{i}{2}h_{\mathrm{ref}}e^{i\mu_s x} + \sigma\frac{\partial\psi}{\partial x}, \quad (3)$$

where $\psi(x,t)$ is the normalized intracavity field amplitude defined in the normalized azimuthal coordinate x, δ is the normalized loss, h_{pmp} (h_{ref}) is the normalized main (reference) pump amplitude, and σ is the normalized detuning of the reference pump from its closest comb-line frequency. By treating the loss and gain terms perturbatively and grouping them together within the term $\epsilon\mathcal{P}(x,t)$, we can rewrite the detuning-normalized MLLE in Eq. (3) as

$$\frac{\partial\psi}{\partial t} = -\frac{i}{2}\psi + \frac{i}{2}\frac{\partial^2\psi}{\partial x^2} + i|\psi|^2\psi + \epsilon\mathcal{P}(x,t), \quad (4)$$

where $\epsilon\mathcal{P}(\psi,x,t) = -\delta\psi + \sigma\partial\psi/\partial x - (i/2)[h_{\mathrm{pmp}} + h_{\mathrm{ref}}e^{i\mu_s x}]$ are the terms we will treat perturbatively and the ϵ coefficient is used to indicate that the terms are small. The MLLE as written in Eq. (4) is convenient for theoretical analysis because it is of the form of a perturbed nonlinear Schrödinger equation, which enables the use of standard soliton perturbation theory to study the impact of the reference pump on the soliton. We therefore assume that the solution is of the form

$$\psi_s(x,t) = A\mathrm{sech}[A(x - x_0)]e^{i\mu_r(x - x_0) - i\phi}, \quad (5)$$

where the parameters $p_j = A, x_0, \mu_r, \phi$ are the soliton amplitude, central position, central frequency (which we also refer to as spectral recoil), and central phase, respectively. We assume that only these four parameters are subject to variation due to the presence of a perturbation. With this assumption, we employ soliton perturbation theory to calculate how x_0 changes with time in the presence of the loss and gain perturbative terms (see the Supplemental Material), and we obtain

$$\frac{dx_0}{dt} = h_{\mathrm{DKS}}^2\mu_r - \sigma + \frac{h_{\mathrm{ref}}\pi^2}{4A^2}\mathrm{sech}\left(\frac{\mu_s\pi}{2A}\right)\tanh\left(\frac{\mu_s\pi}{2A}\right), \quad (6)$$

where $h_{\mathrm{DKS}} = \sqrt{(\pi/A)\int_{-\infty}^{\infty}|\Psi_s(\mu)|^2 d\mu}$ is the normalized soliton energy, $x \leftrightarrow \mu$ are Fourier transform pairs, and $\Psi_s(\mu) = \int_{-\infty}^{\infty}\psi_s(x)e^{-i\mu x}dx$ is the Fourier transform of $\psi_s(x)$. When the soliton is in the KIS regime, Eq. (4) has stationary solutions. Therefore, in KIS, $dx_0/dt = 0$, and Eq. (6) becomes

$$h_{\mathrm{DKS}}^2\mu_r = -\frac{h_{\mathrm{ref}}\pi^2}{4A^2}\mathrm{sech}\left(\frac{\mu_s\pi}{2A}\right)\tanh\left(\frac{\mu_s\pi}{2A}\right) + \sigma,$$
$$h_{\mathrm{DKS}}^2\mu_r = -h_{\mathrm{KIS}}^2\tanh\left(\frac{\mu_s\pi}{2A}\right) + \sigma. \quad (7)$$

We note that $h_{\mathrm{KIS}}^2 = (\pi^2/4A^2)h_{\mathrm{ref}}\mathrm{sech}(\mu_s\pi/2A)$, and h_{KIS} was previously defined as the KIS energy [12,17] equal to the normalized geometric mean of the reference pump energy h_{ref} and the power of the comb tooth where the synchronization occurs $h(\mu_s) = \mathrm{sech}(\mu_s\pi/2A)$. While [17] showed that a spectral recoil can occur with a change in the DKS repetition rate when the reference pump frequency is detuned from the comb-tooth frequency of the unsynchronized DKS ($\sigma \neq 0$),

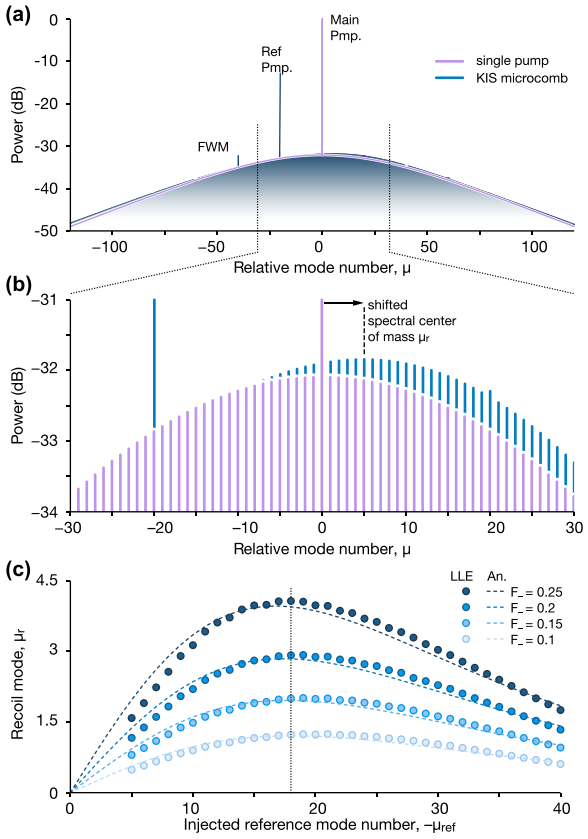


FIG. 2. Self-balancing in a pure quadratic integrated dispersion microresonator. (a) Simulated spectra with (blue) and without (purple) KIS. FWM: four-wave mixing. The parameters from Eq. (1) used in this simulation are $F_{\mathrm{pmp}} = 1.5$, $F_{\mathrm{ref}} = 0.25$, and $\alpha_{\mathrm{pmp}} = 2.5$. (b) Spectral recoil that occurs due to KIS. When the reference pump is used to synchronize the DKS on one side of the spectrum, a spectral recoil occurs, and the spectral center of mass is shifted in the opposite direction. (c) Comparison of simulated and analytically calculated spectral recoil at varying reference pump mode numbers and amplitudes. The simulated spectral recoil (circles) follows the numerically fitted analytical expression in Eq. (7) (dotted lines). The maximal spectral recoil is obtained at the same μ_{ref} for all reference pump amplitudes.

our aim in this section is to conclusively show that the self-balancing phenomenon is more general and that a spectral recoil occurs even without a change in the DKS repetition rate and momentum. Therefore, we consider the case where the reference pump is injected at a frequency exactly equal to the frequency of one of the comb lines, i.e., when $\sigma = 0$. In this case, Eq. (7) shows that there is indeed a spectral recoil ($\mu_r \neq 0$), as shown in Fig. 2(b), even though there is no change in the DKS repetition rate. This results in a behavior similar to the all-optical phase trapping through cavity modulation of a table-top fiber comb, which could be used to counteract the undesirable spectral recoil arising from the Raman effect [39]. Our results present the main advantage of KIS-induced self-balancing as an all-optical phenomenon and therefore compatible with any cavity free spectral range and hence with an integrated DKS platform. This result is significant by itself because it shows that KIS exhibits a spectral recoil without a change in its repetition rate, unlike systems with Raman-induced spectral recoil [21,40] or high-order dispersion [25,31], where a spectral recoil is necessarily associated with a change in the repetition rate. Furthermore, Eq. (7) has the form of a conservation-of-torque equation because it can be written in the form $m_1 l_1 = m_2 l_2$, where $m_1 = h_{\mathrm{DKS}}^2$ and $m_2 = h_{\mathrm{KIS}}^2$ represent masslike quantities and $l_1 = \mu_r$ and $l_2 = -\tanh(\mu_s \pi / 2A)$ represent lengthlike quantities. Therefore, Eq. (7) provides the magnitude of the spectral recoil needed for the DKS to maintain its repetition rate. The right-hand side of Eq. (7) has a distinctive $\mathrm{sech}(\cdot)\tanh(\cdot)$ form, implying that for a given reference pump amplitude, an optimal mode number μ_s exists at which the reference pump can be injected to maximize the recoil and that this optimal mode number is independent of the reference pump amplitude. An important difference from the expression that was derived for the spectral recoil in [18] using the method of moments is that the expression we have derived here is an explicit function of the reference pump mode number and offers testable predictions such as the existence of an optimal mode number, while the expression in [18] is a function of a phase term whose mode-number dependence is unknown and can be obtained only through numerical simulations. To verify the validity of our analytical calculations, we simulate Eq. (2) while fixing all parameters except μ_{ref} and varying μ_{ref} for different values of F_{ref}. The simulated spectral recoil (circles) in [Fig. 2(c)] matches the numerically fit Eq. (7) (dotted lines). We observe that the maximum spectral recoil occurs at the same reference pump mode number for all reference pump amplitudes, thereby validating Eq. (7) and confirming that self-balancing necessitates a redistribution of spectral energy even when the DKS repetition rate remains unchanged.

III. SELF-BALANCING EFFECT IN THE PRESENCE OF A DISPERSIVE WAVE

In Sec. II, we observed analytically and numerically through MLLE simulations that the injection of a reference pump causes the soliton to undergo a spectral recoil to conserve its spectral center of mass without changing the repetition rate, lending credence to the notion of self-balancing. Ultimately, however, we are interested in showing that the self-balancing effect can lead to an increase in DW power as a way to conserve the spectral center of mass. Additionally, we aim to show that an increase in DW power is indeed due to self-balancing and not through simple four-wave mixing between the main and reference pumps. Prior theoretical work on the impact of KIS in systems with high-order dispersion was restricted to numerically studying how the locking range for KIS is modified [18]. However, the dependence of DW power enhancement on the reference pump power and the existence of an optimal injection mode number have not been studied. Since DWs were not present in the simple system with a pure quadratic integrated dispersion that we considered in the previous section, we modify the integrated dispersion to include a small but non-negligible third-order dispersion term. We restrict the present analysis to the regime of weak third-order dispersion, which leads to the formation of a DW relatively far from the center of the soliton spectrum, such that its effects can be treated perturbatively. For larger values, the

DKS dynamics become substantially more intricate [41] and would require a separate treatment that is beyond the scope of this work. Including third-order dispersion modifies Eq. (2), which now becomes

$$\frac{\partial a}{\partial t} = -(1 + i\alpha_{\mathrm{pmp}})a + iD_2\frac{\partial^2 a}{\partial\theta^2} + D_3\frac{\partial^3 a}{\partial\theta^3} + i|a|^2 a + F_{\mathrm{pmp}} + F_{\mathrm{ref}}e^{i[\alpha_{\mathrm{ref}}-\alpha_{\mathrm{pmp}}+D_{\mathrm{int}}(\mu_{\mathrm{ref}})]t+i\mu_{\mathrm{ref}}\theta}, \quad (8)$$

where D_3 is the third-order dispersion coefficient. Normalizing Eq. (8) with respect to the detuning α_{pmp}, we now find

$$\frac{\partial\psi}{\partial t} = -\frac{i}{2}\psi + \frac{i}{2}\frac{\partial^2\psi}{\partial x^2} + i|\psi|^2\psi + \epsilon\mathcal{P}^{3\mathrm{OD}}(x,t), \quad (9)$$

where $\epsilon\mathcal{P}^{3\mathrm{OD}}(x,t)$ contain the terms we treat perturbatively, given by

$$\epsilon\mathcal{P}^{3\mathrm{OD}}(x,t) = -\delta\psi + \beta_3\frac{\partial^3\psi}{\partial x^3} + \sigma\frac{\partial\psi}{\partial x} - \frac{i}{2}h_{\mathrm{pmp}} - \frac{i}{2}h_{\mathrm{ref}}e^{i\mu_s x}, \quad (10)$$

where β_3 is the detuning-normalized third-order dispersion coefficient. We choose the signs of β_3 and μ_s such that the DW mode and the reference pump mode are on opposite sides of the spectrum. In this modified system, there are now two routes for the conservation of the soliton spectral center of mass in the KIS regime—a spectral recoil similar to what was described in the case of a pure quadratic integrated dispersion and also an enhancement of the DW power. That is, the presence of a DW acts as a new degree of freedom for the soliton self-balancing to occur. We first calculate the impact of KIS on the soliton spectral recoil. As a starting point for our perturbative analysis, we assume the soliton ansatz that was derived in [42] and used in [25],

$$\psi_s(x,t) = A\mathrm{sech}[A(x-x_0)]e^{\{i\mu_r^{3\mathrm{OD}}(x-x_0)-3iA\tanh[A(x-x_0)]\}}, \quad (11)$$

where we have applied the transformation $x \to x - \beta_3 t$ to remove the change to the group velocity caused by third-order dispersion and $\mu_r^{3\mathrm{OD}}$ is the soliton central frequency in the presence of third-order dispersion and KIS. Using the same perturbative technique that we used in the previous section but with the modified perturbation in Eq. (10), we obtain an expression for the spectral recoil with third-order dispersion and a reference pump

$$h_{\mathrm{DKS}}^2\mu_r^{3\mathrm{OD}} = \sigma - \frac{h_{\mathrm{ref}}}{4}\frac{\pi^2}{A^2}\mathrm{sech}\left(\frac{\mu_s\pi}{2A}\right)\tanh\left(\frac{\mu_s\pi}{2A}\right) + 2\beta_3A^2, \quad (12)$$

which is identical to Eq. (7) except for the additional term $2\beta_3A^2$, which is the spectral recoil due to the third-order dispersion term. First, we note that Eq. (12) predicts a shift in the soliton spectral center of mass with a magnitude proportional to β_3, which is a result of the change in DKS momentum due to the emission of a DW. Equation (12) also shows that the presence of the reference pump continues to modify the soliton spectral center of mass in a manner identical to what was observed in the simplistic pure-D_2 system that was considered in the previous section. Additionally, Eq. (12) shows that injecting the reference pump at a mode on the opposite side of the spectrum to where the DW is can counteract the recoil due to the DW. This effect provides a KIS-enabled all-optical pathway to suppress unwanted spectral recoil, like those arising through the Raman effect or strong DW emissions. We verified the validity of this effect through MLLE simulations and observed that synchronizing the DKS with a reference pump with sufficiently high power and at a mode on the opposite side of the spectrum from the DW can completely cancel the recoil induced by the DW emission without modifying the DKS repetition rate, as shown in Figs. 3(a) and 3(b). The MLLE simulations also show that the power of the comb teeth increases around the DW mode [Fig. 3(c)]. Having numerically and analytically shown that KIS can lead to a spectral recoil, we next calculate the DW power as a function of the mode number (see the Supplemental Material),

$$\Delta P(\mu_{\mathrm{DW}}) = C(\beta_3,\mu_{\mathrm{DW}})\frac{h_{\mathrm{ref}}\pi^4}{8A^3}\mathrm{sech}\left(\frac{\pi\mu_s}{2A}\right)\tanh\left(\frac{\pi\mu_s}{2A}\right), \quad (13)$$

where $C(\beta_3,\mu_{\mathrm{DW}}) = \beta_3\mu_{\mathrm{DW}}^3\mathrm{sech}(\pi\mu_{\mathrm{DW}}/2A)\tanh(\pi\mu_{\mathrm{DW}}/2A)$ and μ_{DW} is the relative mode number at which the DW is found. Notably, Eq. (13) predicts that the optimal mode number $\mu_{s,\mathrm{opt}}$ for maximizing DW power enhancement is independent of both β_3 and the reference pump amplitude. Using the same parameters as in Fig. 2, we compute the DW power change over a range of μ_s for several reference pump amplitudes, as shown in Fig. 3(d). We find that the numerically computed DW power enhancement agrees well with the numerically fitted analytical expression in Eq. (13) and confirm that $\mu_{s,\mathrm{opt}}$ is independent of the reference pump amplitude. Moreover, because we use the same value of D_2 in Figs. 2 and 3, the optimal mode number for the maximal spectral recoil in Fig. 2 is identical to the optimal mode number for the maximal DW power enhancement in Fig. 3. Since $\mu_{s,\mathrm{opt}} \neq -\mu_{\mathrm{DW}}$, this behavior cannot be explained by simple four-wave mixing between the main and reference pumps. Instead, it identifies self-balancing as the governing mechanism where the conservation of the SCM occurs through a combination of spectral recoil and DW power enhancement. Next, we calculate the change in power of the comb tooth at the mode pumped by the reference pump (see the Supplemental Material),

$$\Delta P(\mu_s) = \beta_3\mu_s^3\frac{h_{\mathrm{ref}}\pi^4}{8A^3}\mathrm{sech}^2\left(\frac{\mu_s\pi}{2A}\right)\tanh^2\left(\frac{\mu_s\pi}{2A}\right). \quad (14)$$

Dividing Eq. (13) by Eq. (14), we obtain

$$\frac{\Delta P(\mu_{\mathrm{DW}})}{\Delta P(\mu_s)} = \frac{\mu_{\mathrm{DW}}^3\mathrm{sech}\left(\frac{\mu_{\mathrm{DW}}\pi}{2A}\right)\tanh\left(\frac{\mu_{\mathrm{DW}}\pi}{2A}\right)}{\mu_s^3\mathrm{sech}\left(\frac{\mu_s\pi}{2A}\right)\tanh\left(\frac{\mu_s\pi}{2A}\right)}, \quad (15)$$

which equals the reference-to-DW conversion efficiency via self-balancing. Rearranging the terms in Eq. (13), we obtain

$$\frac{1}{\mu_{\mathrm{DW}}^3}\cosh\left(\frac{\mu_{\mathrm{DW}}\pi}{2A}\right)\coth\left(\frac{\mu_{\mathrm{DW}}\pi}{2A}\right)\Delta P(\mu_{\mathrm{DW}}) = \frac{1}{\mu_s^3}\cosh\left(\frac{\mu_s\pi}{2A}\right)\coth\left(\frac{\mu_s\pi}{2A}\right)\Delta P(\mu_s). \quad (16)$$

Noting that $(1/x^3)\cosh(x)\coth(x)$ is always a positive quantity and increases monotonically at large $|x|$, we can draw an analogy between Eq. (16) and the law of moments and rewrite Eq. (16) as

$$m(\mu_{\mathrm{DW}})l(\mu_{\mathrm{DW}}) = m(\mu_s)l(\mu_s), \quad (17)$$

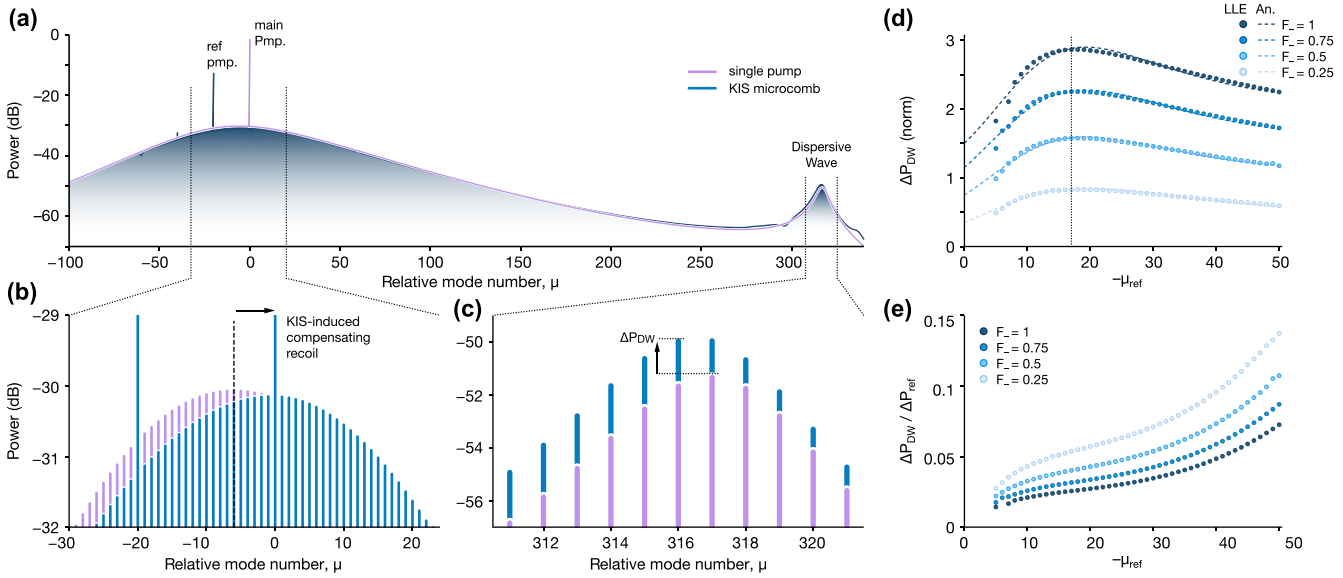


FIG. 3. Demonstration of the self-balancing effect in the presence of a single DW. (a) Comparison of the frequency-comb spectra with (blue) and without (purple) KIS. In the absence of KIS, the peak of the spectrum is offset from $\mu = 0$ due to a spectral recoil resulting from the presence of a DW. When a reference pump is injected at the frequency of the comb line at $\mu_{\text{ref}} = -20$, the soliton enters the KIS regime and experiences a spectral recoil in a manner identical to what was shown in the pure quadratic case. (b) The KIS-induced spectral recoil opposes the recoil due to the DW, and they cancel each other out, leaving the resulting spectrum nearly symmetric around $\mu = 0$. (c) Apart from the spectral recoil, the self-balancing effect leads to a significant increase in the power of the comb lines around the DW mode. (d) Change in the DW power as a function of the mode at which the reference pump is injected for different reference pump powers. The circles show results obtained from the MLLE, and dotted lines are fits to the analytical expression obtained in Eq. (13). A clear peak exists at the same μ_{ref} regardless of the power of the reference pump, and the DW power decreases monotonically away from this peak, clearly demonstrating that the DW enhancement in the presence of the reference pump is not due to simple four-wave mixing between the main and reference pumps. (e) The ratio of the DW power and the reference pump power as a function of the reference pump mode number, indicating the efficiency of DW enhancement due to the self-balancing effect. The ratio increases monotonically with μ_{ref}, in agreement with Eq. (16).

where $m(\mu_n) = \Delta P(\mu_n)$ represents a masslike quantity and $l(\mu_n) = (1/\mu_n^3)\cosh(\mu_n \pi/2A)\coth(\mu_n \pi/2A)$ represents a lengthlike quantity. To verify the validity of Eq. (17), we simulate the MLLE [Eq. (8)] with a fixed reference pump power and calculate the ratio in Eq. (15) for increasing μ_s. We observe that the ratio becomes larger at high μ_s, as shown in Fig. 3(e) and predicted by Eq. (17).

IV. DISPERSIVE WAVE ENHANCEMENT WITH QUARTIC DISPERSION

Having established the self-balancing behavior in purely quadratic and cubic integrated dispersion systems, we now extend our analysis to a resonator with an experimentally realistic and desirable quartic dispersion that supports two distinct DWs on either side of the main pump frequency. This system provides a practical platform for achieving broadband, octave-spanning frequency combs suitable for self-referencing applications, where high power at both spectral extremes is desirable to realize a sufficient signal-to-noise ratio in f_{ceo} detection. While dispersion engineering can introduce DWs at either end of the soliton spectrum, their powers at higher frequencies are limited due to inefficient out-coupling. It was previously shown in [12] that achieving KIS by injecting the reference pump at the low-frequency DW resulted in a substantial increase in the power of the high-frequency DW despite the DW mode numbers being asymmetric with respect to the main pump. Since the DWs are sufficiently far from the center of the DKS spectrum, injecting the reference pump at the low-frequency DW enables efficiently achieving KIS because the comb-tooth frequency is very close to the corresponding resonance frequency. The self-balancing mechanism that KIS enables offers a means to redistribute soliton energy, enabling selective enhancement of the weaker high-frequency DW without perturbing the soliton repetition rate. The condition that the DWs are far from the center of the DKS spectrum is important because it ensures that the DKS remains in the anomalous dispersion regime, avoiding the near-zero-GVD regime [43,44] where the DKS dynamics are fundamentally altered [45]. This ensures that the perturbation theory developed for cubic dispersion in the previous section continues to govern the DW enhancement, with the key distinction that the reference pump now couples energy to the system more efficiently. We numerically model the behavior using the MLLE [Eq. (1)] with an integrated dispersion up to fourth-order terms, thereby generating a microcomb that exhibits two DWs unequally spaced from the primary pump frequency, as shown in Fig. 4(a). When the reference pump is injected at a frequency that coincides with the frequency of the low-frequency DW, the soliton enters the KIS regime, fixing its repetition rate while enforcing the conservation of its spectral center of mass. Due to self-balancing, the soliton reallocates its energy by enhancing the high-frequency DW power, as shown in Fig. 4(a). Next, we consider how the

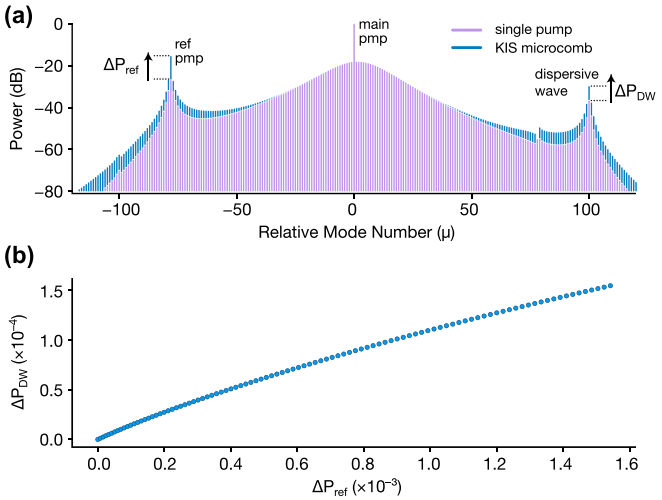


FIG. 4. Numerical demonstration of DW power enhancement due to self-balancing. (a) Numerically calculated spectra with (blue) and without (purple) KIS, demonstrating that the injection of the reference pump at the low-frequency DW leads to a proportional increase in the high-frequency DW power ΔP_{DW} on the other side of the spectrum. (b) The change in the high-frequency DW power is linearly proportional to the change in the comb-tooth power where the reference pump is injected, as predicted analytically.

high-frequency DW power depends on the reference pump power. Equation (13) predicts that the change in DW power is linearly proportional to the change in the power of the mode pumped by the reference pump. In the MLLE, we calculate the change in the high-frequency DW power as a function of the change in the reference pump power, as shown in Fig. 4(b). We observe that the DW power follows the linear relationship that is predicted by the soliton-perturbation-theory model, further confirming that the self-balancing mechanism operates consistently across dispersion regimes.

V. CONCLUSION

We theoretically and numerically demonstrated KIS-induced self-balancing of dissipative Kerr solitons. Through perturbative analysis of the multipump Lugiato-Lefever equation and corresponding numerical simulations, we showed that a soliton can conserve its spectral center of mass by dynamically redistributing energy between different regions of its spectrum. In the simplest quadratic-dispersion system, this manifests as a spectral recoil on the opposite side of the optical spectrum from the reference pump. The self-balancing-induced recoil can be harnessed to all-optically compensate for undesirable sources of spectral recoil such as those arising due to the Raman effect without requiring external components that may not be chip compatible [39]. Extending our analysis to systems that include higher-order dispersion, we showed that this same self-balancing mechanism transfers energy into a DW on the opposite side of the spectrum, leading to measurable power enhancement without changing the repetition rate. For a quartic-dispersion resonator supporting two DWs, we showed that synchronizing the soliton at the low-frequency DW results in significant self-balancing-induced enhancement of the high-frequency DW power. The observed linear scaling of DW power with reference pump power is a direct signature of self-balancing and distinguishes the process from simple four-wave mixing. These results establish soliton self-balancing as a universal mechanism governing the energy flow in DKSs operating in the KIS regime. Interestingly, our approach could be extended to a multi-DKS state within the same resonator. In addition to reorganizing the multisoliton state in the optical-lattice trap generated by beating between the main and reference pump lasers [46], we expect self-balancing to act collectively on the intracavity field rather than independently on each soliton. This collective action could produce a combined effect on the extracted microcomb, opening new avenues for optimizing metrological microcomb sources. Beyond revealing a new form of nonlinear cavity equilibria and intracavity energy dynamics, self-balancing provides an all-optical pathway to engineer coherent spectral broadening of chip-scale octave-spanning microcombs whose spectral properties cannot be conveniently altered postfabrication.

ACKNOWLEDGMENTS

P.S. and C.M. acknowledge support from National Center for Manufacturing Sciences (Cooperative Agreements No. 2022138-142232 and No. 2023200-142386 as subawards from DOD Cooperative Agreements No. HQ0034-20-2-0007 and No. HQ0034-24-2-0001) and from the National Institute of Standards and Technology (Grant No. 60NANB24D106). G.M. and K.S. acknowledge partial funding support from the Space Vehicles Directorate of the Air Force Research Laboratory and the NIST-on-a-chip program of the National Institute of Standards and Technology. We thank Shao-Chien Ou and Lida Xu for insightful feedback.

G.M., C.M., and K.S. have submitted a provisional patent application based on aspects of the work presented in this paper.

DATA AVAILABILITY

The data that support the findings of this article are not publicly available because of legal restrictions preventing unrestricted public distribution. The data are available from the authors upon reasonable request.

[1] B. Stern, X. Ji, Y. Okawachi, A. L. Gaeta, and M. Lipson, Battery-operated integrated frequency comb generator, Nature (London) **562**, 401 (2018).

[2] J. Liu, G. Huang, R. N. Wang, J. He, A. S. Raja, T. Liu, N. J. Engelsen, and T. J. Kippenberg, High-yield, wafer-scale fabrication of ultralow-loss, dispersion-engineered silicon nitride photonic circuits, Nat. Commun. **12**, 2236 (2021).

[3] S.-C. Ou, A. O. Antohe, L. G. Carpenter, G. Moille, and K. Srinivasan, 300 mm wafer-scale SiN platform for broadband soliton microcombs compatible with alkali atomic references, Opt. Lett. **50**, 5578 (2025).

[4] D. T. Spencer *et al.*, An optical-frequency synthesizer using integrated photonics, Nature (London) **557**, 81 (2018).

[5] Z. L. Newman *et al.*, Architecture for the photonic integration of an optical atomic clock, Optica **6**, 680 (2019).

[6] B. Corcoran, A. Mitchell, R. Morandotti, L. K. Oxenløwe, and D. J. Moss, Optical microcombs for ultrahigh-bandwidth communications, Nat. Photon. **19**, 451 (2025).

[7] A. Dutt, C. Joshi, X. Ji, J. Cardenas, Y. Okawachi, K. Luke, A. L. Gaeta, and M. Lipson, On-chip dual-comb source for spectroscopy, Sci. Adv. **4**, e1701858 (2018).

[8] J. Riemensberger, A. Lukashchuk, M. Karpov, W. Weng, E. Lucas, J. Liu, and T. J. Kippenberg, Massively parallel coherent laser ranging using a soliton microcomb, Nature (London) **581**, 164 (2020).

[9] G. Huang, E. Lucas, J. Liu, A. S. Raja, G. Lihachev, M. L. Gorodetsky, N. J. Engelsen, and T. J. Kippenberg, Thermorefractive noise in silicon-nitride microresonators, Phys. Rev. A **99**, 061801(R) (2019).

[10] T. E. Drake, J. R. Stone, T. C. Briles, and S. B. Papp, Thermal decoherence and laser cooling of Kerr microresonator solitons, Nat. Photon. **14**, 480 (2020).

[11] H. R. Telle, G. Steinmeyer, A. Dunlop, J. Stenger, D. Sutter, and U. Keller, Carrier-envelope offset phase control: A novel concept for absolute optical frequency measurement and ultrashort pulse generation, Appl. Phys. B **69**, 327 (1999).

[12] G. Moille, J. Stone, M. Chojnacky, R. Shrestha, U. A. Javid, C. Menyuk, and K. Srinivasan, Kerr-induced synchronization of a cavity soliton to an optical reference, Nature (London) **624**, 267 (2023).

[13] G. Moille, S. K. Sridhar, P. Shandilya, A. Dutt, C. Menyuk, and K. Srinivasan, Toward chaotic group velocity hopping of an on-chip dissipative Kerr soliton, Phys. Rev. Lett. **135**, 133802 (2025).

[14] S. Sun, M. W. Harrington, F. Tabatabaei, S. Hanifi, K. Liu, J. Wang, B. Wang, Z. Yang, R. Liu, J. S. Morgan, S. M. Bowers, P. A. Morton, K. D. Nelson, A. Beling, D. J. Blumenthal, and X. Yi, Microcavity Kerr optical frequency division with integrated SiN photonics, Nat. Photon. **19**, 637 (2025).

[15] G. Moille, P. Shandilya, J. Stone, C. Menyuk, and K. Srinivasan, All-optical noise quenching of an integrated frequency comb, Optica **12**, 1020 (2025).

[16] H. Taheri, A. B. Matsko, and L. Maleki, Optical lattice trap for Kerr solitons, Eur. Phys. J. D **71**, 153 (2017).

[17] T. Wildi, A. Ulanov, N. Englebert, T. Voumard, and T. Herr, Sideband injection locking in microresonator frequency combs, APL Photonics **8**, 120801 (2023).

[18] H. Taheri, A. B. Matsko, and K. A. Wiesenfeld, Dynamics of dissipative cavity solitons in a lattice trap, Laser Photonics Rev. **19**, 2500257 (2025).

[19] Q.-F. Yang, X. Yi, K. Y. Yang, and K. Vahala, Spatial-mode-interaction-induced dispersive waves and their active tuning in microresonators, Optica **3**, 1132 (2016).

[20] V. Brasch, M. Geiselmann, T. Herr, G. Lihachev, M. H. P. Pfeiffer, M. L. Gorodetsky, and T. J. Kippenberg, Photonic chip–based optical frequency comb using soliton Cherenkov radiation, Science **351**, 357 (2016).

[21] C. Milián, A. V. Gorbach, M. Taki, A. V. Yulin, and D. V. Skryabin, Solitons and frequency combs in silica microring resonators: Interplay of the Raman and higher-order dispersion effects, Phys. Rev. A **92**, 033851 (2015).

[22] M. Karpov, H. Guo, A. Kordts, V. Brasch, M. H. P. Pfeiffer, M. Zervas, M. Geiselmann, and T. J. Kippenberg, Raman self-frequency shift of dissipative Kerr solitons in an optical microresonator, Phys. Rev. Lett. **116**, 103902 (2016).

[23] X. Yi, Q.-F. Yang, X. Zhang, K. Y. Yang, X. Li, and K. Vahala, Single-mode dispersive waves and soliton microcomb dynamics, Nat. Commun. **8**, 14869 (2017).

[24] A. C. Triscari, A. Tusnin, A. Tikan, and T. J. Kippenberg, Quiet point engineering for low-noise microwave generation with soliton microcombs, Commun. Phys. **6**, 318 (2023).

[25] N. Akhmediev and M. Karlsson, Cherenkov radiation emitted by solitons in optical fibers, Phys. Rev. A **51**, 2602 (1995).

[26] Y. Okawachi, M. R. E. Lamont, K. Luke, D. O. Carvalho, M. Yu, M. Lipson, and A. L. Gaeta, Bandwidth shaping of microresonator-based frequency combs via dispersion engineering, Opt. Lett. **39**, 3535 (2014).

[27] M. Erkintalo, Y. Q. Xu, S. G. Murdoch, J. M. Dudley, and G. Genty, Cascaded phase matching and nonlinear symmetry breaking in fiber frequency combs, Phys. Rev. Lett. **109**, 223904 (2012).

[28] S. Coen, H. G. Randle, T. Sylvestre, and M. Erkintalo, Modeling of octave-spanning Kerr frequency combs using a generalized mean-field Lugiato–Lefever model, Opt. Lett. **38**, 37 (2013).

[29] W. Weng, R. Bouchand, E. Lucas, and T. J. Kippenberg, Polychromatic Cherenkov radiation induced group velocity symmetry breaking in counterpropagating dissipative Kerr solitons, Phys. Rev. Lett. **123**, 253902 (2019).

[30] G. Moille, X. Lu, J. Stone, D. Westly, and K. Srinivasan, Fourier synthesis dispersion engineering of photonic crystal microrings for broadband frequency combs, Commun. Phys. **6**, 144 (2023).

[31] A. V. Cherenkov, V. E. Lobanov, and M. L. Gorodetsky, Dissipative Kerr solitons and Cherenkov radiation in optical microresonators with third-order dispersion, Phys. Rev. A **95**, 033810 (2017).

[32] D. J. Kaup, Perturbation theory for solitons in optical fibers, Phys. Rev. A **42**, 5689 (1990).

[33] H. A. Haus and Y. Lai, Quantum theory of soliton squeezing: A linearized approach, J. Opt. Soc. Am. B **7**, 386 (1990).

[34] T. Georges, Perturbation theory for the assessment of soliton transmission control, Opt. Fiber Technol. **1**, 97 (1995).

[35] J. P. Mizrahi, L. Courtright, P. Shandilya, C. R. Menyuk, and O. Gat, Soliton synchronization in microresonators with a modulated pump, Phys. Rev. E **109**, 064204 (2024).

[36] A. Leshem, S. Akter, L. Courtright, P. Shandilya, C. R. Menyuk, and O. Gat, Dynamics of interacting cavity solitons, Phys. Rev. E **113**, 014207 (2026).

[37] See Supplemental Material at http://link.aps.org/supplemental/10.1103/921d-nf7h for a review of soliton perturbation theory and derivations of the analytical expressions for the spectral recoil in a pure-D_2 microresonator and for the dispersive-wave enhancement in the presence of third-order dispersion, which also includes Ref. [38].

[38] C. Milián and D. V. Skryabin, Soliton families and resonant radiation in a micro-ring resonator near zero group-velocity dispersion, Opt. Express **22**, 3732 (2014).

[39] N. Englebert, C. Simon, C. Mas Arabí, F. Leo, and S.-P. Gorza, Dynamics of driven dissipative temporal solitons in an intracavity phase trap, Light: Sci. Appl. **15**, 117 (2026).

[40] X. Yi, Q.-F. Yang, K. Y. Yang, and K. Vahala, Theory and measurement of the soliton self-frequency shift and efficiency in optical microcavities, Opt. Lett. **41**, 3419 (2016).

[41] P. Parra-Rivas, D. Gomila, F. Leo, S. Coen, and L. Gelens, Third-order chromatic dispersion stabilizes Kerr frequency combs, Opt. Lett. **39**, 2971 (2014).

[42] Y. Kodama and A. Hasegawa, Nonlinear pulse propagation in a monomode dielectric guide, IEEE J. Quantum Electron. **23**, 510 (1987).

[43] M. H. Anderson, W. Weng, G. Lihachev, A. Tikan, J. Liu, and T. J. Kippenberg, Zero dispersion Kerr solitons in optical microresonators, Nat. Commun. **13**, 4764 (2022).

[44] Z. Xiao, T. Li, M. Cai, H. Zhang, Y. Huang, C. Li, B. Yao, K. Wu, and J. Chen, Near-zero-dispersion soliton and broadband modulational instability Kerr microcombs in anomalous dispersion, Light: Sci. Appl. **12**, 33 (2023).

[45] Z. Li, Y. Xu, C. Todd, G. Xu, S. Coen, S. G. Murdoch, and M. Erkintalo, Observations of existence and instability dynamics of near-zero-dispersion temporal Kerr cavity solitons, Phys. Rev. Res. **3**, 043207 (2021).

[46] P. Shandilya, S.-C. Ou, J. Stone, C. Menyuk, M. Erkintalo, K. Srinivasan, and G. Moille, All-optical azimuthal trapping of dissipative Kerr multi-solitons for relative noise suppression, APL Photon. **10**, 016104 (2025).

Supplementary Information: Dissipative Kerr Soliton Self-Balancing from Kerr-Induced Synchronization

Pradyoth Shandilya,[1] Kartik Srinivasan,[2,3,*] Curtis Menyuk,[1] and Grégory Moille[2,3,†]

[1] *University of Maryland, Baltimore County, Baltimore, MD, USA*
[2] *Microsystems and Nanotechnology Division, National Institute of Standards and Technology, Gaithersburg, USA*
[3] *Joint Quantum Institute, NIST/University of Maryland, College Park, USA*

(Dated: October 3, 2026)

S.1 Review of soliton perturbation theory

In this section, we will review how soliton perturbation theory can be used to calculate the impact of perturbations on soliton parameters. The nonlinear Schrödinger equation (NLSE) can be written as

$$\frac{\partial \psi}{\partial t} \equiv N(\psi) = -\frac{i}{2}(A^2+\mu_r^2)\psi + \mu_r \frac{\partial \psi}{\partial x} + \frac{i}{2}\frac{\partial^2 \psi}{\partial x^2} + i|\psi|^2\psi, \tag{S.1.1}$$

which admits stationary soliton solutions of the form

$$\psi_s(x,t) = A\,\mathrm{sech}[A(x-x_0)]e^{i[\mu_r(x-x_0)]-i\phi}, \tag{S.1.2}$$

where the parameters $p_j = \{A, x_0, \mu_r, \text{and } \phi\}$ are the soliton amplitude, central position, central frequency (or spectral recoil), and phase respectively. The linearized operator of the NLSE, $\mathcal{L} = \delta N/\delta\Psi|_{\Psi_s}$ is

$$\mathcal{L} = \begin{pmatrix} -\frac{i}{2}(A^2+\mu_r^2) + \mu_r\frac{\partial}{\partial x} + \frac{i}{2}\frac{\partial^2}{\partial x^2} + 2i|\psi_s|^2 & i\psi_s^2 \\ -i(\psi_s^*)^2 & \frac{i}{2}(A^2+\mu_r^2) + \mu_r\frac{\partial}{\partial x} - \frac{i}{2}\frac{\partial^2}{\partial x^2} - 2i|\psi_s|^2 \end{pmatrix} \tag{S.1.3}$$

and $\Psi = (\psi, \psi^*)$. Since the soliton solution in Eq. (S.1.2) has four free parameters, Eq. (S.1.3) has four h zero eigenvalues,

$$\psi_A = \frac{\psi_s}{A}\{1 - A(x-x_0)\tanh[A(x-x_0)]\} \tag{S.1.4a}$$
$$\psi_{\mu_r} = i(x-x_0)\psi_s \tag{S.1.4b}$$
$$\psi_\phi = -i\psi_s \tag{S.1.4c}$$
$$\psi_{x_0} = -\frac{\partial \psi_s}{\partial x} = \psi_s\{-i\mu_r + A\tanh[A(x-x_0)]\} \tag{S.1.4d}$$

each of which corresponds to a perturbation of one of the four soliton parameters. To find the adjoint eigenfunctions of Eq. (S.1.4), we will first write the adjoint of Eq. (S.1.3). The adjoint matrix $\mathcal{L}^\dagger$ is given by

$$\mathcal{L}^\dagger = \begin{pmatrix} \frac{i}{2}(A^2+\mu_r^2) + \mu_r\frac{\partial}{\partial x} - \frac{i}{2}\frac{\partial^2}{\partial x^2} - 2i|\psi_s|^2 & i\psi_s^2 \\ -i(\psi_s^*)^2 & -\frac{i}{2}(A^2+\mu_r^2) + \mu_r\frac{\partial}{\partial x} + \frac{i}{2}\frac{\partial^2}{\partial x^2} + 2i|\psi_s|^2 \end{pmatrix}. \tag{S.1.5}$$

The generalized eigenfunctions of Eq. (S.1.5) that satisfy the inner product relation $\langle \overline{\Psi}_m, \Psi_n \rangle = \delta_{mn}$ for the eigenfunctions of Eq. (S.1.3) are

$$\overline{\psi}_A = \psi_s \tag{S.1.6a}$$
$$\overline{\psi}_{\mu_r} = i\psi_s\tanh[A(x-x_0)] \tag{S.1.6b}$$
$$\overline{\psi}_\phi = -\frac{\psi_s}{A}\{i + \mu_r(x-x_0) - iA(x-x_0)\tanh[A(x-x_0)]\} \tag{S.1.6c}$$
$$\overline{\psi}_{x_0} = (x-x_0)\frac{\psi_s}{A}. \tag{S.1.6d}$$

* kartik.srinivasan@nist.gov

† gmoille@umd.edu

Next, we assume that the Lugiato-Lefever equation (LLE) is of the form

$$\frac{\partial\psi}{\partial t} = -\frac{i}{2}\psi + \frac{i}{2}\frac{\partial^2\psi}{\partial x^2} + i|\psi|^2\psi + \epsilon\chi(x,t,\psi) \tag{S.1.7}$$

where $\chi(x,t,\psi)$ contains all loss and gain (pump) terms, and any other perturbation whose impact we want to analyze that cannot otherwise be handled analytically. We can rewrite Eq. (S.1.7) in the form of Eq. (S.1.1) as

$$\frac{\partial\psi}{\partial t} = N(\psi) - \mu_r\frac{\partial\psi}{\partial x} + \frac{i}{2}(A^2+\mu_r^2-1)\psi + \epsilon\chi(x,t,\psi), \tag{S.1.8}$$

and equivalently in matrix form as

$$\frac{\partial\Psi}{\partial t} = N(\Psi) - \mu_r\frac{\partial\Psi}{\partial x} + \frac{i}{2}(A^2+\mu_r^2-1)I\Psi + \epsilon\mathcal{P}(x,t,\Psi), \tag{S.1.9}$$

where I is the identity matrix. In general, we can write the solution of the LLE as a sum of the NLSE solution in Eq. (S.1.2) and a perturbative correction term

$$\Psi(x) = \Psi_s(p_j) + \epsilon\Delta\Psi(x,t), \tag{S.1.10}$$

Substituting this in Eq. (S.1.9), for any p_j, we obtain

$$\begin{aligned}\Psi_{p_j}\frac{dp_j}{dt} + \epsilon\frac{\partial\epsilon\Delta\Psi}{\partial t} =& \epsilon\mathcal{L}\Delta\Psi + \mu_r\Psi_{x_0} - \mu_r\frac{\partial\Delta\Psi}{\partial x} - \frac{1}{2}(A^2+\mu_r^2-1)I\Psi_\phi \\ &+ \epsilon\frac{i}{2}(A^2+\mu_r^2-1)I\Delta\Psi + \epsilon\mathcal{P}.\end{aligned} \tag{S.1.11}$$

In Eq. (S.1.11), we have made use of the fact that $\partial\psi_s/\partial x = -\psi_{x_0}$ and $i\psi_s = -\psi_\phi$ to simplify the form of the equation. To obtain the equation of motion of any of the free parameters, we simply have to take the inner product of Eq. (S.1.11) with respect to the corresponding adjoint eigenfunction and note that $\langle\overline{\Psi}_m, \Delta\Psi\rangle = 0$ and $\langle\overline{\Psi}_m, \Psi_n\rangle = \delta_{m,n}$. Substituting x_0 and μ_r in Eq. (S.1.11), we obtain the equations of motion for the central position and central frequency,

$$\frac{dx_0}{dt} = \mu_r + \epsilon\langle\overline{\Psi}_{x_0}, \mathcal{P}\rangle \tag{S.1.12a}$$

$$\frac{d\mu_r}{dt} = \epsilon\langle\overline{\Psi}_{\mu_r}, \mathcal{P}\rangle \tag{S.1.12b}$$

S.2 Derivation of analytical expression for spectral recoil in pure-D_2 microresonator

Here, we derive the self-balancing equation for a purely quadratic integrated dispersion microresonator, given in Eq. (7) in the main text. The soliton dynamics in a dual-pumped microresonator can be modeled using the loss-normalized multi-pump Lugiato-Lefever equation (MLLE)[1,2]

$$\begin{aligned}\frac{\partial a}{\partial t} =& -(1+i\alpha_{\text{pmp}})\,a + i\sum_\mu D_{\text{int}}(\mu)A(\mu)e^{i\mu\theta} + i|a|^2a \\ &+ F_{\text{pmp}} + F_{\text{ref}}e^{i(\alpha_{\text{ref}}-\alpha_{\text{pmp}}+D_{\text{int}}(\mu_{\text{ref}}))t+i\mu_{\text{ref}}\theta},\end{aligned} \tag{S.2.1}$$

where a is the intracavity field amplitude, A is its Fourier transform, t is time, θ is the azimuthal coordinate, α_{pmp} (α_{ref}) is the detuning of the primary (reference) pump with corresponding amplitudes F_{pmp} (F_{ref}), D_{int} is the integrated dispersion as a function of the relative mode number μ, and μ_s is the relative mode number of the reference pump. Considering only up to second-order dispersion, Eq. (S.2.1) reduces to

$$\begin{aligned}\frac{\partial a}{\partial t} =& -(1+i\alpha_{\text{pmp}})\,a + iD_2\frac{\partial^2 a}{\partial\theta^2} + i|a|^2a \\ &+ F_{\text{pmp}} + F_{\text{ref}}e^{i(\alpha_{\text{ref}}-\alpha_{\text{pmp}}+D_{\text{int}}(\mu_{\text{ref}}))t+i\mu_{\text{ref}}\theta},\end{aligned} \tag{S.2.2}$$

where D_2 is the second-order dispersion coefficient. Using the following change of variables in Eq. (S.2.2) which represents a frame of reference where the pump fields are stationary[2]

$$\theta + \frac{\alpha_{\text{ref}} + \alpha_{\text{pmp}} + D_{\text{int}}(\mu_{\text{ref}})}{\mu_{\text{ref}}}t = \theta', t = t', \tag{S.2.3}$$

we obtain the autonomous MLLE

$$\begin{aligned}\frac{\partial a}{\partial t} =& -(1+i\alpha_{\mathrm{pmp}})\,a + iD_2\frac{\partial^2 a}{\partial\theta^2} + i|a|^2 a \\ &- \frac{\alpha_{\mathrm{ref}} - \alpha_{\mathrm{pmp}} + D_{\mathrm{int}}(\mu_{\mathrm{ref}})}{\mu_{\mathrm{ref}}}\frac{\partial\psi}{\partial\theta} \\ &+ F_{\mathrm{pmp}} + F_{\mathrm{ref}}e^{i\mu_{\mathrm{ref}}\theta},\end{aligned} \tag{S.2.4}$$

where we have dropped the primes for convenience. The loss-normalized MLLE is convenient for physical intuition and numerical simulations because it directly relates to experimentally tunable parameters, namely the pump amplitudes (F_{pmp} and F_{ref}) and pump detunings (α_{pmp} and α_{ref}). However, Eq. (S.2.1) cannot be directly used to analytically study the impact of the reference pump on the soliton spectral energy dynamics. To facilitate analytical treatment of the energy dynamics, we normalize Eq. (S.2.4) with respect to the main pump detuning and obtain[3]

$$\begin{aligned}\frac{\partial\psi}{\partial t} =& -\left(\delta + \frac{i}{2}\right)\psi + \frac{i}{2}\frac{\partial^2\psi}{\partial x^2} + i|\psi|^2\psi \\ &- \frac{i}{2}h_{\mathrm{pmp}} - \frac{i}{2}h_{\mathrm{ref}}e^{i\mu_s x} + \sigma\frac{\partial\psi}{\partial x},\end{aligned} \tag{S.2.5}$$

where $\psi = a/\sqrt{2\alpha_{\mathrm{pmp}}}$ is the normalized intracavity field amplitude, $\delta = 1/2\alpha_{\mathrm{pmp}}$ is the normalized loss, $h_{\mathrm{pmp,ref}} = iF_{\mathrm{pmp,ref}}/\sqrt{2}\alpha_{\mathrm{pmp}}^{3/2}$ is the normalized main (reference) pump amplitude, $t = t \times 2\alpha_{\mathrm{pmp}}$ is the normalized time, $x = \sqrt{2\alpha_{\mathrm{pmp}}}\theta$, and σ is the normalized detuning of the reference pump. In the large main pump detuning limit ($\alpha_{\mathrm{pmp}} \to \infty$), the normalized loss ($\delta$), and gain terms ($h_{\mathrm{pmp}}$ and h_{ref}) become small, and can be treated as perturbations to the NLSE. Therefore, we can re-write Eq. (S.2.5) as

$$\frac{\partial\psi}{\partial t} = -\frac{i}{2}\psi + \frac{i}{2}\frac{\partial^2\psi}{\partial x^2} + i|\psi|^2\psi + \epsilon\chi, \tag{S.2.6}$$

where $\epsilon\chi = -\delta\psi + \sigma\partial\psi/\partial x - (i/2)(h_{\mathrm{main}} + h_{\mathrm{ref}}e^{i\mu_s x})$, and the coefficient ϵ is used to denote that the terms in $\epsilon\chi$ are small. Eq. (S.2.6) is exactly the same as Eq. (S.1.7), and therefore we can use Eq. (S.1.12) to obtain the equations of motion. For the central position, we obtain

$$\begin{aligned}\frac{\partial x_0}{\partial t} &= \frac{\pi}{A}M_S\mu_r - \sigma - \frac{h_{\mathrm{ref}}}{2}\sin(\mu_s x_0)\int_{-\infty}^{\infty} x\,\mathrm{sech}(Ax)\sin((\mu_s+\mu_r)x)dx \\ &= \frac{\pi}{A}M_s\mu_r - \sigma - \frac{h_{\mathrm{ref}}\pi^2}{4A^2}\,\mathrm{sech}\left[\frac{(\mu_s+\mu_r)\pi}{2A}\right]\tanh\left[\frac{(\mu_s+\mu_r)\pi}{2A}\right]\end{aligned} \tag{S.2.7}$$

Since the spectral recoil is typically much smaller than the reference pump mode number, we assume that $\mu_s \gg \mu_r$ and simplify Eq. (S.2.7) as

$$\frac{\partial x_0}{\partial t} = \frac{\pi}{A}M_s\mu_r - \sigma - \frac{h_{\mathrm{ref}}\pi^2}{4A^2}\,\mathrm{sech}\left(\frac{\mu_s\pi}{2A}\right)\tanh\left(\frac{\mu_s\pi}{2A}\right). \tag{S.2.8}$$

The coefficient $(\pi/A)M_S$ is equal to one (which we retain for the sake of clarity) and $M_S = \int_{-\infty}^{\infty}|\mathcal{F}(\psi(x))|^2 d\mu$ is the soliton's spectral mass. In the KIS regime, the soliton solution is stationary. Therefore, setting $\partial x_0/\partial t = 0$, we obtain

$$\frac{\pi}{A}M_S\mu_r = \frac{h_{\mathrm{ref}}\pi^2}{4A^2}\,\mathrm{sech}\left(\frac{\mu_s\pi}{2A}\right)\tanh\left(\frac{\mu_s\pi}{2A}\right) + \sigma, \tag{S.2.9}$$

which is Eq. (7) in the main text.

S.3 Derivation of analytical expression for dispersive wave enhancement in the presence of third-order dispersion

In this section, we derive the enhancement in the dispersive wave (DW) power due to self-balancing (Eq. (13) in the main text). The MLLE in the presence of third-order dispersion is

$$\frac{\partial\psi}{\partial t} = -\frac{i}{2}\psi + \frac{i}{2}\frac{\partial^2\psi}{\partial x^2} + i|\psi|^2\psi + \epsilon\mathcal{P}^{\mathrm{3OD}}(x,t), \tag{S.3.1}$$

where $\epsilon\mathcal{P}^{3\mathrm{OD}}(x,t)$ contain the terms we treat perturbatively, given by

$$\epsilon\mathcal{P}^{3\mathrm{OD}}(x,t) = -\delta\psi + \beta_3\frac{\partial^3\psi}{\partial x^3} + \sigma\frac{\partial\psi}{\partial x} - \frac{i}{2}h_{\mathrm{pmp}} - \frac{i}{2}h_{\mathrm{ref}}e^{i\mu_s x}, \tag{S.3.2}$$

where β_3 is the detuning-normalized third-order dispersion coefficient. To use soliton perturbation theory, we use the expression derived in[4] as the soliton solution ansatz in the presence of third-order dispersion

$$\psi_s^{3\mathrm{OD}}(x,t) = A\,\mathrm{sech}[A(x-\beta_3 t)]e^{i\beta_3\{2A^2(x-\beta_3 t)-3A\tanh[A(x-\beta_3 t)]\}}. \tag{S.3.3}$$

First, we calculate the impact of KIS on the spectral recoil μ_r in Eq. (S.3.1). Using the ansatz in Eq. (S.3.3) and subtituting Eq. (S.3.2) in Eq. (S.1.12), and setting $dx_0/dt = 0$, we obtain

$$\mu_r^{3\mathrm{OD}} = \sigma + \frac{h_{\mathrm{ref}}}{4}\frac{\pi^2}{A^2}\,\mathrm{sech}\Big(\frac{\mu_s\pi}{2A}\Big)\tanh\Big(\frac{\mu_s\pi}{2A}\Big) + 2\beta_3A^2, \tag{S.3.4}$$

where the term $2\beta_3A^2$ is the spectral recoil due to third-order dispersion and the remaining terms are due to the self-balancing effect. Having obtained the spectral recoil with KIS in the presence of third-order dispersion, we modify the ansatz in Eq. (S.3.3) to include $\mu_r^{(3\mathrm{OD})}$ explicitly,

$$\begin{aligned}\psi_s^{3\mathrm{OD}} &= A\,\mathrm{sech}(Ax')\exp\Big[i\mu_r^{(3\mathrm{OD})}x' - 3A\epsilon\beta_3\tanh(Ax)\Big] \\ &\approx A\,\mathrm{sech}(Ax)[1 + i\mu_r^{3\mathrm{OD}}x - 3iA\epsilon\beta_3\tanh(Ax)].\end{aligned} \tag{S.3.5}$$

where $x' = x - x_0$. We will now use the modified ansatz in Eq. (S.3.5) to calculate the position and power of the DW in the presence of third-order dispersion following[4]. DWs occur when the soliton is in resonance with a linear wave, i.e., when the soliton wavenumber is equal to that of a linear dispersive wave. Assuming that the DW is a linear wave of the form $e^{i(k_l t+\mu x)}$ and substituting it into Eq. (S.1.1), we obtain

$$k_l(\mu) = -\frac{1}{2}\mu^2 - \beta_3\mu^3. \tag{S.3.6}$$

Equating the wavenumber obtained in Eq. (S.3.6) to the soliton wavenumber ($k_s = A^2/2$), we obtain the DW phase-matching condition

$$\beta_3\mu_{\mathrm{DW}}^3 + \frac{1}{2}\mu_{\mathrm{DW}}^2 + \frac{A^2}{2} = 0. \tag{S.3.7}$$

This phase-matching condition, obtained here by equating the soliton and linear-wave wavenumbers, is equivalent to the dispersive-wave phase-matching condition derived by Milián and Skryabin[5]. Both follow from the same soliton-radiation resonance and differ only in the choice of normalization and notation. Solving Eq. (S.3.7) to first order, we obtain the DW position

$$\mu_{\mathrm{DW}} = -\frac{1}{2\beta_3}. \tag{S.3.8}$$

We assume that the solution of Eq. (S.3.1) is of the form $\psi(x,t) = \psi_s^{3\mathrm{OD}}(x,t) + f(x,t)$, where $f(x,t)$ is the DW. Linearizing Eq. (S.3.1) with respect to $f(x,t)$, we obtain

$$\frac{\partial f}{\partial t} - \frac{i}{2}\frac{\partial^2 f}{\partial x^2} + i\beta_3\frac{\partial^3 f}{\partial x^3} - 2i|\psi_s^{3\mathrm{OD}}|^2 f - i(\psi_s^{3\mathrm{OD}})^2 f = -i\beta_3\frac{\partial^3\psi_s^{3\mathrm{OD}}}{\partial x^3}. \tag{S.3.9}$$

Assuming that the DW has a fixed azimuthal form that is phase-matched with the soliton, we can substitute the ansatz $f(x,t) = r(x)e^{ik_s t}$ in Eq. (S.3.9) and take the Fourier transform to obtain

$$R(\mu) = \frac{\mathcal{F}[\beta_3\partial^3\psi_s^{3\mathrm{OD}}/\partial x^3]}{k_l(\mu) - k_s} \equiv \frac{P(\mu)}{k_l(\mu) - k_s}, \tag{S.3.10}$$

where $R(\mu)$ is the DW in the normalized mode number domain, $\mathcal{F}$ is the Fourier transform operator, and $P(\mu)$, which is proportional to the DW power, is

$$P(\mu, h_{\mathrm{ref}}) = -i\beta_3\mu^3\left[\pi\,\mathrm{sech}\Big(\frac{\pi\mu}{2A}\Big) + \mu^{3\mathrm{OD}}(\beta_3, h_{\mathrm{ref}})\frac{\pi^2}{2A}\,\mathrm{sech}\Big(\frac{\pi\mu}{2A}\Big)\tanh\Big(\frac{\pi\mu}{2A}\Big) - 3\beta_3\pi\mu\,\mathrm{sech}\Big(\frac{\pi\mu}{2A}\Big)\right]. \tag{S.3.11}$$

Subsituting Eq. (S.3.4) with and without h_{ref} in Eq. (S.3.11), we obtain the DW power enhancement in KIS

$$\Delta P(\mu_{\mathrm{DW}}) = C(\beta_3, \mu_{\mathrm{DW}}) \frac{h_{\mathrm{ref}} \pi^4}{8A^3} \operatorname{sech}\left(\frac{\pi \mu_s}{2A}\right) \tanh\left(\frac{\pi \mu_s}{2A}\right), \tag{S.3.12}$$

where $C(\beta_3, \mu_{\mathrm{DW}}) = \beta_3 \mu_{\mathrm{DW}}^3 \operatorname{sech}\left[(\pi \mu_{\mathrm{DW}})/(2A)\right] \tanh\left[(\pi \mu_{\mathrm{DW}})/(2A)\right]$.

[1] H. Taheri, A. B. Matsko, and L. Maleki, Optical lattice trap for Kerr solitons, The European Physical Journal D **71**, 153 (2017).

[2] G. Moille, P. Shandilya, J. Stone, C. Menyuk, and K. Srinivasan, All-optical noise quenching of an integrated frequency comb, Optica **12**, 1020 (2025).

[3] J. P. Mizrahi, L. Courtright, P. Shandilya, C. R. Menyuk, and O. Gat, Soliton synchronization in microresonators with a modulated pump, Physical Review E **109**, 064204 (2024).

[4] N. Akhmediev and M. Karlsson, Cherenkov radiation emitted by solitons in optical fibers, Physical Review A **51**, 2602 (1995).

[5] C. Milián and D. V. Skryabin, Soliton families and resonant radiation in a micro-ring resonator near zero group-velocity dispersion, Optics Express **22**, 3732 (2014)